



Inhibition of human Na_v1.5 sodium channels by strychnine and its analogs

Chunhua Yuan^{a,1}, Lirong Sun^{a,1}, Meng Zhang^a, Shuji Li^a, Xuemin Wang^a,
Tianming Gao^a, Xinhong Zhu^{a,b,*}

^a Department of Anatomy and Neurobiology, Southern Medical University, Guangzhou 510515, China

^b School of Traditional Chinese Medicine, Southern Medical University, Guangzhou 510515, China

ARTICLE INFO

Article history:

Received 11 January 2011

Accepted 9 May 2011

Available online 14 May 2011

Keywords:

Na_v1.5 channel

Alkaloid

Strychnine

Icajine

Arrhythmias

ABSTRACT

Strychnine and brucine from the seeds of the plant *Strychnos nux vomica* have been shown to have interesting pharmacological effects on several neurotransmitter receptors. In this study, we have characterized the pharmacological properties of strychnine and its analogs on human Na_v1.5 channels to assess their potential therapeutic advantage in certain arrhythmias. Among the eight alkaloids, only strychnine and icajine exhibited inhibition potency on the Na_v1.5 channel with the half-maximum inhibition (IC₅₀) values of 83.1 μM and 104.6 μM, respectively. Structure–function analysis indicated that the increased bulky methoxy groups on the phenyl ring or the negatively charged oxygen atom may account for this lack of inhibition on the Na_v1.5 channel. Strychnine and icajine may bind to the channel by cation–π interactions. The substitution with a large side chain on the phenyl ring or the increased molecular volume may alter the optimized position for the compound close to the binding sites of the channel. Strychnine and icajine bind to the Na_v1.5 channel with a new mechanism that is different from TTX and local anesthetics. They bind to the outer vestibule of the channel pore with fast association and dissociation rates at resting state. Strychnine and icajine had little effect on steady-state fast inactivation but markedly shifted the slow inactivation of Na_v1.5 currents toward more hyperpolarized potentials. The property of icajine influencing slow-inactivated state of Na_v1.5 channel would be potential therapeutic advantages in certain arrhythmias.

© 2011 Elsevier Inc. All rights reserved.

1. Introduction

Na_v1.5, the cardiac isoform of the voltage-gated sodium channels (VGSCs), is critical to heart excitability and conduction. The Na_v1.5 channel protein that is in humans is encoded by the SCN5A gene, and the current of Na_v1.5 is tetrodotoxin (TTX)-resistant [1–4]. The inward sodium current (*I*_{Na}) through open Na_v channels during the action potential plateau will counter the effects of the increased K⁺ efflux, thereby slowing or delaying repolarization and increasing action potential durations [5]. Therefore, changes in the probability that Na_v channels are open at voltages corresponding to the plateau could markedly affect action potential waveforms in ventricular cells. Voltage-dependent inactivation of Na_v1.5, a consequence of voltage-dependent activation, is characterized by at least two distinguishable kinetic components: an initial rapid component (fast inactivation) and a

slower component (slow inactivation). Ion-channel blocking drugs that inhibit peak *I*_{Na} in the ventricle were associated with increased mortality in the cardiac arrhythmia suppression trial [6]. However, blockage of the slow inactivating component of *I*_{Na} might be a useful antiarrhythmic target [7]. This was highlighted by reports that mutations in sodium channels that produced a slowing of inactivation were responsible for some serious clinical arrhythmias [8] and that blockage of the currents is a useful therapeutic intervention in some long QT cases [9–11]. Thus, drugs that behave with a preference for the slow-inactivated state might be good candidates for finding safer sodium blockers that are useful as antiarrhythmics.

Nux vomica, the dried seed of *Strychnos nux vomica* L., which is a moderate-sized tree from the family *Loganiaceae* that is grown extensively in southern Asian countries, has been effectively used in Traditional Chinese Medicine for the treatment of blood circulatory problem and rheumatic pain [12]. Alkaloids are the main bioactive chemicals in *nux vomica* and are responsible for the pharmacological and toxic effects exerted by *nux vomica*. Strychnine and brucine, two dominating monomeric bisindole alkaloids in *nux vomica*, are deadly poisons; thus, *Nux vomica* must be processed before being used as a medicine [13]. During the processing, part of the intrinsic alkaloids, such as strychnine and

* Corresponding author at: Department of Anatomy and Neurobiology, Southern Medical University, Guangzhou 510515, China. Tel.: +86 20 61647112; fax: +86 20 61648216.

E-mail address: zhuxh@fimmu.com (X. Zhu).

¹ These authors contributed equally to this paper.

brucine, transform into their isoforms (e.g., isostrychnine and isobrucine) or nitrogen oxidative derivatives (e.g., strychnine N-oxide and brucine N-oxide), which possess more or equally potent pharmacological effects compared to their parent compounds without having toxic side effects [14]. Additionally, some alkaloid fractions with low content, such as icajine and novacine, are extracted from the plant and have similar structures as strychnine. Together, all of these alkaloids share the common structural feature of one or more phenolic rings with VGSC-blocking drugs, such as lidocaine, which has cardioprotective efficacy [15]. Therefore, we hypothesized that these alkaloids may inhibit I_{Na} expressed specific in cardiac muscle and function as cardioprotective drugs.

In this study, strychnine and its analogs have been characterized pharmacologically on human embryonic kidney tsA201 cells that are transfected with the human $Na_v1.5$ subtype and ventricular myocytes. Among the eight alkaloids (mentioned above), strychnine and icajine exhibited inhibitory effects on the $Na_v1.5$ channel and behaved as slow-inactivated state-preferring drugs. This study provided new insight into the structure–activity relationships for the alkaloid strychnine and its analogs on the voltage-gated sodium channels.

2. Methods

2.1. Alkaloids preparation

Strychnine, brucine, strychnine N-oxide and brucine N-oxide were purchased from Sigma–Aldrich (St. Louis, MO, USA) as standards. Unless otherwise indicated, all compounds were purchased from Sigma–Aldrich. Isobrucine, isostrychnine, icajine and novacine were isolated from the seeds of *S. nux-vomica*. Briefly, the seeds of *S. nux vomica* (0.9 kg) were fried for 3 min at 235 °C in a peanut oil bath. The oil was wiped off the surface of the seeds. The fried seeds were powdered and macerated for 48 h with aqueous ammonia (conc. NH_3 $H_2O:H_2O$, 1:9, v/v; 1.7 L) at room temperature. The mixture was percolated with the same solution, and the percolate was concentrated to 1 L under reduced pressure. The concentration was then extracted with $CHCl_3$. The residue was repeated three times with the same method. Combined $CHCl_3$ phase was evaporated to dryness in vacuo to give a $CHCl_3$ extract. The extract was dissolved in 8% citric acid aqueous solution (aqu.), and the aqu. was adjusted to pH 9–10 with 60% Na_2CO_3 . The aqu. was extracted with $CHCl_3$ five times. The combined $CHCl_3$ solution was evaporated under reduced pressure to give a residue. A portion of the residue (16 g) was subjected to column chromatography over a silica gel column, eluting with a three gradient solvent system of hexane: $CHCl_3$:EtOH:Et₂NH (10:8:0.5:0.3, 5:8:0.5:0.3, 10:8:2.5:0.3, v/v), $CHCl_3$:MeOH (10:1, 5:1, v/v), and MeOH to give five fractions (Fr. 1–Fr. 5). Each fraction was subjected to column chromatography, preparative thin-layer chromatography to give the following compounds: icajine and novacine from Fr. 1, strychnine and brucine from Fr. 2, isostrychnine from Fr. 3, strychnine N-oxide and brucine N-oxide from Fr. 4 and isobrucine from Fr. 5. The structures of separating strychnine, brucine, strychnine N-oxide and brucine N-oxide were determined by thin-layer chromatography as compared to the standards. The structures of icajine, novacine, isostrychnine and isobrucine were elucidated by analysis of 1D NMR spectroscopic data. All of these compounds were identified by high-performance gel permeation chromatography with a purity >95%.

2.2. Cell culture and transfection

Culture medium, serum, antibiotics and Lipofectamine 2000 were obtained from Invitrogen (Paisley, USA). Human embryonic kidney tsA201 cells, a simian virus (SV-40)-transformed derivative

of HEK-293 cells, were maintained at 37 °C in a humidified 5% CO_2 incubator (Thermo Scientific, NC, USA) in culture medium (Dulbecco's Modified Eagle's Medium supplemented with 10% fetal calf serum, 100 U/ml penicillin and 100 U/ml streptomycin). Confluent cells (50–70%) were plated onto a 24-well cell culture Plate 3–4 h before transfection. The tsA-201 cells were transfected with 0.9 μ g of a mix of *SCN5A* cDNA ($Na_v1.5$), *SCN1B* cDNA ($Na_v\beta1$) and *SCN2B* cDNA ($Na_v\beta2$) in equi-molar ratios, together with 0.1 μ g of enhanced green fluorescent protein cDNA using the Lipofectamine 2000 and following the manufacturer's instructions. *SCN5A*, *SCN1B* and *SCN2B* were kind gifts from Dr. Robert S. Kass (Columbia University, New York NY, USA). Cells were trypsinized 24 h after transfection and plated on poly-D-lysine-coated coverslips for recording.

2.3. Preparation of ventricular myocytes

Animal studies were conducted in accordance with the Chinese Council on Animal Care Guidelines. Ventricular myocytes were isolated from 1-day-old Sprague-Dawley rats of either sex by enzymatic dissociation as described previously [16] and modified. Briefly, the heart was rapidly removed via thoractomy after subcutaneous injection of sodium pentobarbital. Ventricles were cut into 1–2-mm cubes and dissociated by agitation (100 rpm) at 37 °C for 10 min in Hank's solution containing 0.125% trypsin. The cellular suspensions were pelleted by centrifugation at 1000 rpm for 5 min. Cells were resuspended in culture medium, containing Dulbecco's modified Eagle's medium/Ham's F-12 medium (Invitrogen, Burlington, OH) and 10% fetal bovine serum (Gibco, USA), and stand for 90 min, then shifted on to 12 mm circle coverslips in 24-well plate. Plate was maintained in a humidified incubator containing 5% CO_2 , 95% air at 37 °C and culture medium was refreshed daily. The ventricular myocytes growing for 48 h on glass coverslips were used for electrophysiological studies.

2.4. Electrophysiology

$Na_v1.5$ currents were recorded from tsA-201 cells with green fluorescent signal. Whole-cell voltage-clamp recording was performed with the Axopatch 200B (Axon Instruments, Foster City, CA, USA). All voltage protocols were applied using pCLAMP 8 software (Axon) and a Digidata 1322A (Axon). Currents were amplified, low pass filtered (2 kHz) and sampled at 10 kHz. Recording patch pipettes were fire-polished to a resistance of 3–5 M Ω . For tsA201 cells recording, the internal solution contained (mM): CsCl 135, NaCl 10, and HEPES 5, adjusted to pH 7.2 with CsOH, and the bath solution contained (mM): NaCl 50, $MgCl_2$ 1, $CaCl_2$ 1.8, CsCl 5, KCl 5, D-Glucose 25, Tetraethylammonium-Cl 70, and HEPES 5, adjusted to pH 7.4 with NaOH. For ventricular myocytes recording, the internal solution contained (mM): CsF 120, NaCl 10, MgATP 5, EGTA 10, Glucose 11, and HEPES 10, adjusted to pH 7.2 with CsOH, and the bath solution contained (mM): NaCl 30, Choline chloride 110, $MgCl_2$ 1, KCl 5.4, NaH_2PO_4 0.33, and HEPES 10, adjusted to pH 7.4 with NaOH. Compounds were prepared as 100 mM stock solutions in dimethyl sulfoxide (DMSO) (Sigma) and diluted to the desired concentration in perfusion solution. The maximum DMSO concentration used was 0.5% and had no effect on current amplitude. All experiments were performed at room temperature (22–25 °C). Series resistance was compensated to 80%, with a 10 μ s lag time. Data were leak-subtracted on-line using a P/4 protocol and analyzed using pClamp V8.0 (Axon).

2.5. Data analysis

Experimental data were acquired and analyzed by the programs Clampfit 8.0 (Axon) and Sigmaplot (Sigma, USA). All data are

presented as the mean \pm standard error (S.E.), and n is the number of independent experiments. Dose–response curves to determine IC_{50} values were fitted using the following form of the Hill equation:

$$y = \frac{1 - (1 - f_{\max})}{1 + ([x]/IC_{50})^{nH}}, \quad (1)$$

where x is the drug dose, nH is the Hill coefficient (slope parameter), and IC_{50} is the half-maximum inhibitory concentration.

The time constants were determined by fitting time course data with the single exponential decay function:

$$y = Ae^{-kx} + C, \quad (2)$$

where x is the time, A is the normalized current value before application of drug (usually 1.0), and C is the final normalized current value following blockage by the drug. The time constant (τ) was determined from the inverse of the rate constant k .

Steady-state inactivation of sodium channels was obtained using the Boltzmann equation:

$$\frac{I}{I_{\max}} = \frac{1}{[1 + \exp(V - V_{1/2})/k]} \quad (3)$$

where $V_{1/2}$ is the potential for half maximum inactivation, k is the slope factor, and V is the test potential.

3. Results

3.1. Blockage of the $Na_v1.5$ channel by strychnine and its analogs

In this study, we first examined the effects of strychnine and its analogs on the human $Na_v1.5$ subtype. Fig. 1A summarized the

chemical structure of the analogs examined in this study. Brucine has two more methoxy groups on the phenyl ring compared to strychnine, and the introduction of an oxygen atom in the N-19 position yielded the compounds strychnine N-oxide and brucine N-oxide (Fig. 1A, left). Breaking of the C12–O bond of strychnine and brucine produced isostrychnine and isobrucine, respectively (Fig. 1A, middle). Icajine and novacine share the same structure with only the little difference of two methoxy group substitutions on the phenyl ring (Fig. 1A, right). The inhibitory effects of the analogs on $Na_v1.5$ channels were assessed by a step depolarization to -30 mV for 50 ms from a holding potential of -90 mV. As shown in Fig. 1B, at the concentration of 200 μ M, strychnine and icajine reduced $Na_v1.5$ currents by about $78.5 \pm 3.2\%$ and $70 \pm 4.1\%$ ($n = 5$), respectively, whereas no significant inhibition effect was detected for the other six analogs.

3.2. Effects of strychnine and icajine on the $Na_v1.5$ channel

The effects of strychnine and icajine at concentrations ranging from 10 μ M to 500 μ M were further measured on the human $Na_v1.5$ subtype. The currents were elicited by a 50-ms depolarization to -30 mV from a holding potential of -90 mV every 5 s. The inhibition effects of strychnine and icajine were in a concentration-dependent manner. Fig. 2 shows the fitting of the dose–response curves with the Hill equation, which yielded the IC_{50} values of 83.1 ± 5.2 μ M for strychnine and 104.6 ± 8.1 μ M for icajine ($n = 5$). To examine whether the depolarization of the membrane is a requirement for the binding of strychnine and icajine to the $Na_v1.5$ channel, we compared the kinetics for the onset of inhibition when depolarizations are applied from a negative holding voltage at 1 Hz, 0.5 Hz, or not at all. As shown in Fig. 3A and B, the kinetics for the onset of inhibition by either strychnine or icajine was unaffected by

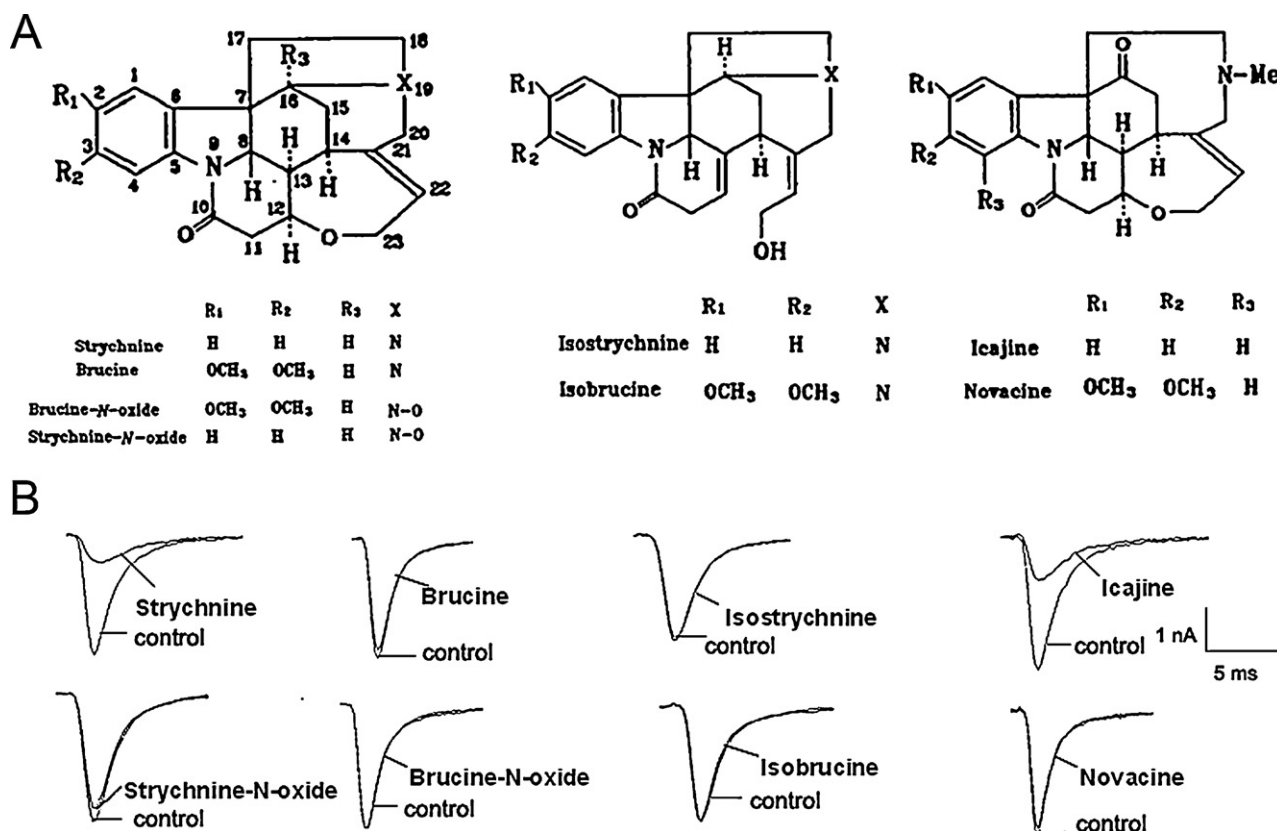


Fig. 1. (A) Chemical structures of strychnine and its analogs. Structures show differences in the phenyl ring substitution. (B) Effects of the eight alkaloids on $Na_v1.5$ channels expressed in Human embryonic kidney tsA201 cells. Current traces were induced by a 50-ms depolarized potential of -30 mV from a holding potential of -90 mV. All of the compounds were applied at a concentration of 200 μ M.

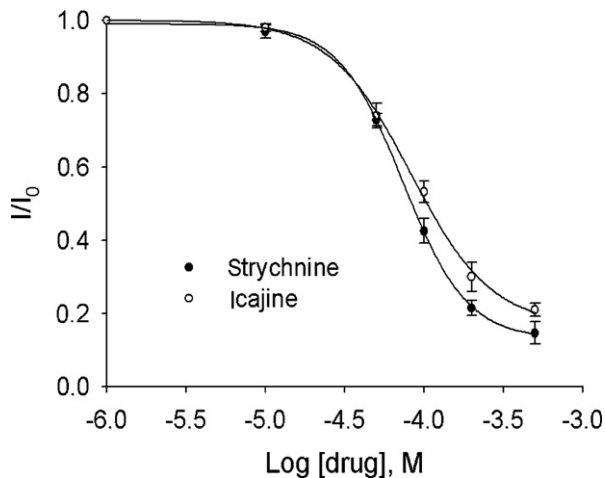


Fig. 2. Dose dependent inhibition of $\text{Na}_v1.5$ channels by strychnine (filled circles) and icajine (open circles). The solid line through the data is a fit of the Hill function. Each point is the mean \pm S.E. for 5 cells.

changing the frequency of depolarization. Moreover, the extent of inhibition is indistinguishable when the channel was held at negative voltages with or without depolarization while the compounds and channel equilibrate. These results suggest that both strychnine and icajine can bind to a closed state of the $\text{Na}_v1.5$ channels. Furthermore, the inhibition kinetics of strychnine and icajine on $\text{Na}_v1.5$ channels were characterized. At the concentration of $200 \mu\text{M}$, both strychnine and icajine produced a rapid inhibition (the time constants for inhibition were $\tau \approx 4.6 \pm 0.1 \text{ s}$ for strychnine and $\tau \approx 6.3 \pm 0.2 \text{ s}$ for icajine, $n = 5$) that was readily reversible. The time constants were

$16.5 \pm 1.8 \text{ s}$ for strychnine and $15.9 \pm 1.2 \text{ s}$ for icajine upon removal of the compounds (Fig. 3C and D).

3.3. Effects of strychnine and icajine on the activation and steady-state inactivation kinetics of $\text{Na}_v1.5$ channels

Next, we examined the effects of strychnine and icajine on channel activation. The current–voltage relationship was determined with a 50 ms voltage step, ranging from -80 to $+60 \text{ mV}$ in steps of 10 mV from a holding potential of -90 mV at 2 s intervals. The currents were initially elicited at -50 mV , and the peak of the current–voltage relationship was -30 mV for the control. Strychnine and icajine reduced the current amplitudes at all potentials, but they did not shift the current–voltage relationships (Fig. 4A and B). To further investigate the mechanism underlying the inhibition, we characterized the effects of strychnine and icajine on steady-state inactivation of $\text{Na}_v1.5$ channels. For steady-state fast inactivation, 50-ms pre-pulses from -130 mV to -30 mV in steps of 10 mV were used, followed by a 50-ms test pulse to -30 mV ($V_h = -130 \text{ mV}$). For steady-state slow inactivation, 9-s pre-pulses from -130 mV to -30 mV in steps of 10 mV were used, followed by a 100-ms pulse to -130 mV to remove fast inactivation, and then a 50-ms test pulse to -30 mV ($V_h = -130 \text{ mV}$). Strychnine ($150 \mu\text{M}$) and icajine ($200 \mu\text{M}$) had little effect on fast inactivation ($V_{1/2}$, from $-77.8 \pm 1.2 \text{ mV}$ for the control to $-74.6 \pm 1.5 \text{ mV}$ and $-75.5 \pm 1.1 \text{ mV}$ for strychnine and icajine, respectively, $n = 7$) (Fig. 4C), but markedly shifted the slow inactivation of $\text{Na}_v1.5$ currents toward more hyperpolarized potentials, indicated by the fact that the $V_{1/2}$ were shifted to $-82.8 \pm 2.1 \text{ mV}$ for strychnine and $-103.9 \pm 1.7 \text{ mV}$ for icajine ($n = 5$) (Fig. 4D), whereas in the control, only $39.2 \pm 3.4\%$ of the

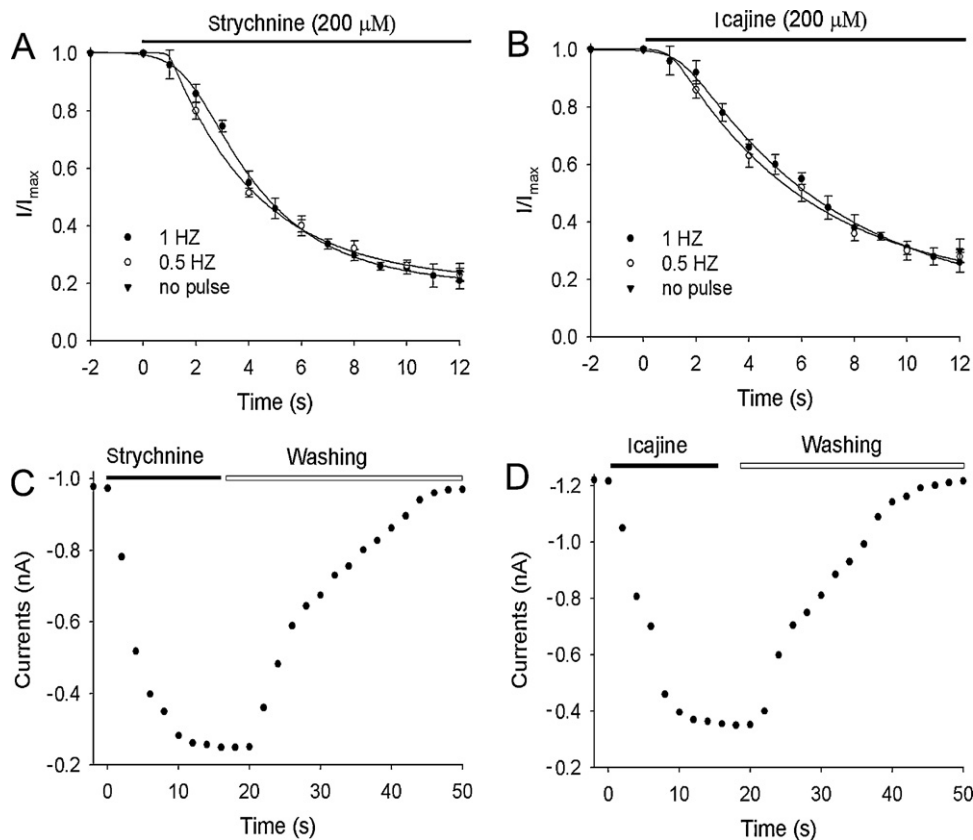


Fig. 3. Inhibition kinetics of strychnine and icajine on $\text{Na}_v1.5$ currents. (A) and (B) Time course for inhibition by strychnine and icajine with different pulse frequencies. No pulse indicates that no pulse was applied for the first 12 s after compound treatment on $\text{Na}_v1.5$ channels. (C) and (D) On- and off-rates determined following application of strychnine ($200 \mu\text{M}$) and icajine ($200 \mu\text{M}$) and wash-out with drug-free external solution ($n = 5$). Currents were elicited by depolarization to -30 mV from a holding potential of -90 mV . Data points were fitted to a single exponential function.

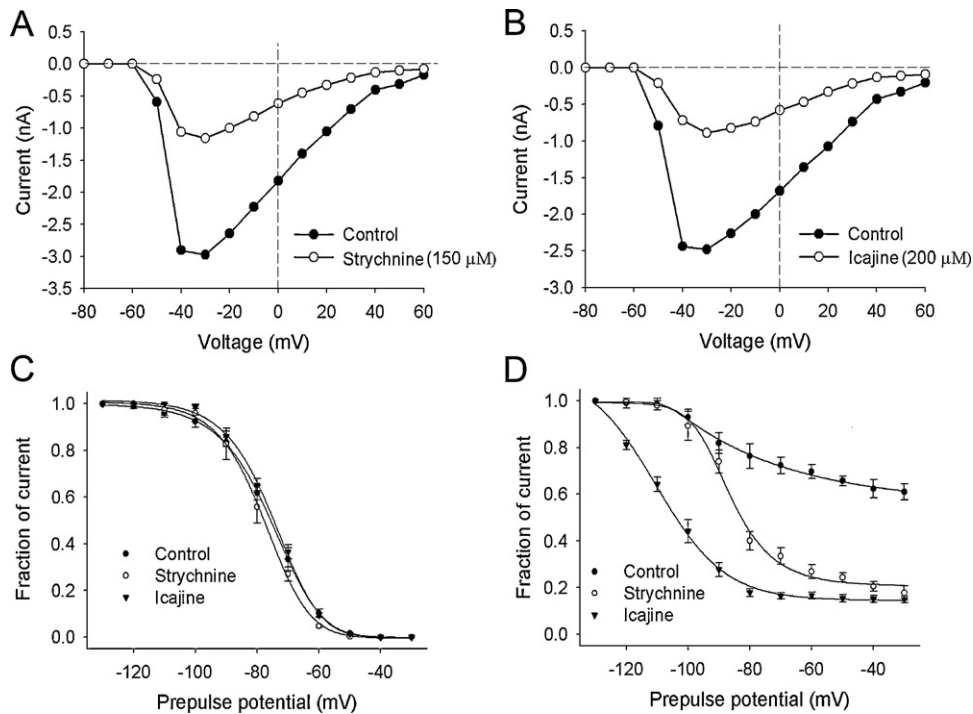


Fig. 4. Effects of strychnine and icajine on the steady-state activation and inactivation of $\text{Na}_v1.5$ channels. (A) and (B) Steady-state current–voltage relationships of $\text{Na}_v1.5$ currents. Current traces were evoked by a 50-ms depolarization to various test potentials from a holding potential of -90 mV. (C) Strychnine ($150 \mu\text{M}$) and icajine ($200 \mu\text{M}$) had no effect on steady-state fast inactivation of $\text{Na}_v1.5$ channels. Currents were induced by 50-ms pre-pulses from -130 mV to -30 mV in steps of 10 mV, followed by a 50-ms test pulse to -30 mV. The data points (mean \pm S.E., $n = 7$) were fitted to equation of $I/I_{\text{max}} = 1/[1 + \exp(V - V_{1/2})/k]$. (D) Effects of strychnine ($150 \mu\text{M}$) and icajine ($200 \mu\text{M}$) on the steady-state slow inactivation of $\text{Na}_v1.5$ currents. For steady-state slow inactivation, 9-s pre-pulses from -130 mV to -30 mV in steps of 10 mV were used, followed by a 100-ms pulse to -130 mV to remove fast inactivation, and then by a 50-ms test pulse to -30 mV.

$\text{Na}_v1.5$ channels were induced to slow inactivation at membrane potentials positive to -30 mV.

3.4. Effects of strychnine and icajine on the inactivation kinetics of sodium channels in ventricular myocytes

To determine whether strychnine and icajine functionally inhibited the $\text{Na}_v1.5$ current in native cells, we further investigated the effect of strychnine and icajine on the inactivation kinetics of sodium channels in ventricular myocytes. As shown in Fig. 5A, strychnine ($150 \mu\text{M}$) and icajine ($200 \mu\text{M}$) had little effect on fast inactivation ($V_{1/2}$, from -71.8 ± 1.3 mV for the control to -73.5 ± 1.6 mV and -74.3 ± 1.2 mV for strychnine and icajine, respectively, $n = 5$), but shifted the slow inactivation of sodium channels toward hyperpolarized potentials. The $V_{1/2}$ were shifted to

-76.7 ± 2.6 mV for strychnine and -92.8 ± 2.1 mV for icajine ($n = 5$) (Fig. 5B), whereas in the control, only $35.5 \pm 3.1\%$ of the sodium channels were induced to slow inactivation at the potential of -30 mV. These results were consistent with the previous results tested on $\text{Na}_v1.5$ subtype.

3.5. Effects of strychnine and icajine on the recovery of $\text{Na}_v1.5$ channels

To determine the influence of strychnine and icajine on the recovery of $\text{Na}_v1.5$ channels from fast inactivation, a two-pulse protocol was used. A pre-pulse from -90 to -30 mV for 100 ms was applied to inactivate all channels. Then, the cells were held at -90 mV for a variable period (1 – 60 ms) to allow for the channels to recover, and the proportion of recovered channels was assessed

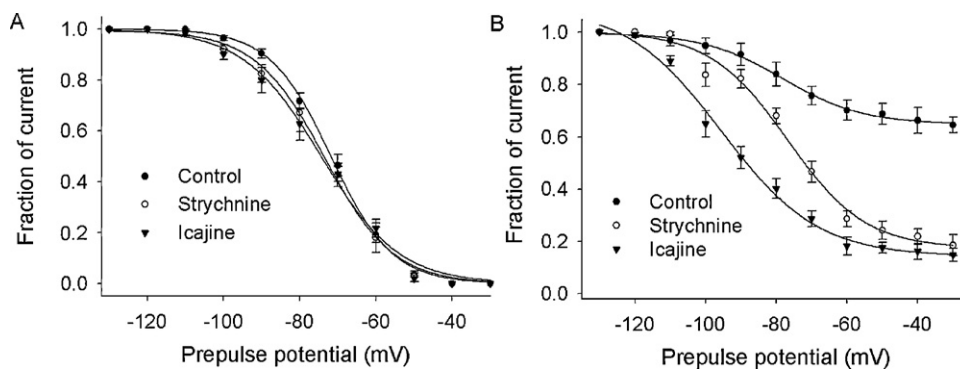


Fig. 5. Effects of strychnine and icajine on the steady-state inactivation of sodium channels in cardiac myocytes. (A) Strychnine ($150 \mu\text{M}$) and icajine ($200 \mu\text{M}$) had no effect on steady-state fast inactivation of the sodium channels. Currents were induced by 100-ms pre-pulses from -130 mV to -30 mV in steps of 10 mV, followed by a 20-ms test pulse to -30 mV. The data points (mean \pm S.E., $n = 5$) were fitted to equation of $I/I_{\text{max}} = 1/[1 + \exp(V - V_{1/2})/k]$. (B) Effects of strychnine ($150 \mu\text{M}$) and icajine ($200 \mu\text{M}$) on the steady-state slow inactivation of the sodium currents. For steady-state slow inactivation, 5-s pre-pulses from -130 mV to -30 mV in steps of 10 mV were used, followed by a 50-ms pulse to -130 mV to remove fast inactivation, and then by a 20-ms test pulse to -30 mV.

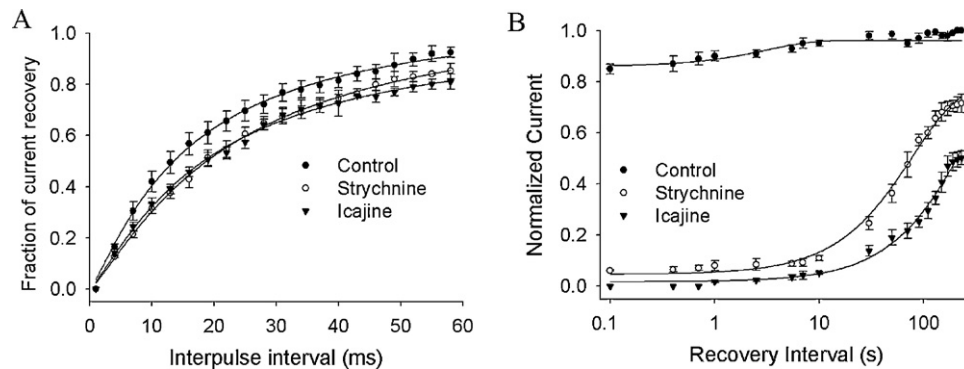


Fig. 6. Strychnine and icajine slow the recovery of the $\text{Na}_v1.5$ channel. (A) Recovery from fast inactivation was assessed using a two-pulse protocol. A pre-pulse from -90 to -30 mV for 100 ms was applied to inactivate all channels. Cells were then held at -90 mV for a variable period (1 – 60 ms) to allow channels to recover, and then the proportion of recovered channels was assessed with a voltage step to -30 mV. The current amplitude is normalized to the peak current recorded in the pre-pulse. (B) Recovery from strychnine ($300 \mu\text{M}$) and icajine ($300 \mu\text{M}$) block at -30 mV for 5 s were measured after a variable recovery interval at -90 mV. A 10 -ms test pulse at -30 mV was used to evoke available currents. The current amplitude was normalized to the peak current amplitude without drug. Data points represent the mean \pm S.E. Each smooth line was fitted by a single-exponential function.

with a voltage step to -30 mV. The currents were normalized to the peak current at the last time point. Recovery data were fitted by a single exponential function. As a control, the half-recovery time was 13.69 ± 0.82 ms for $\text{Na}_v1.5$ channels. However, strychnine and icajine at a half-maximum inhibition concentration delayed channel recovery, with the half-recovery time increasing to 20.27 ± 1.32 ms and 18.36 ± 1.21 ms, respectively ($n = 5$, $P < 0.05$) (Fig. 6A). Furthermore, the recovery time course of $\text{Na}_v1.5$ channels from strychnine and icajine block was investigated. As shown in Fig. 6B, the recovery from strychnine ($300 \mu\text{M}$) block was slow with the time constant of 78.74 ± 6.15 s ($n = 5$), whereas the recovery was much slower in the presence of icajine ($300 \mu\text{M}$) with the time constant of 277.67 ± 15.36 s ($n = 5$, $P < 0.05$).

3.6. Binding domain analysis for strychnine and icajine on $\text{Na}_v1.5$ channels

Strychnine and icajine neither changed the activation threshold nor delayed sodium current inactivation, indicating that they acted

more like pore-blocking drugs. To further test this hypothesis, we first analyzed the competing inhibition effect of icajine and JZTX-1, a site 3 toxin which delays sodium current inactivation [17], on $\text{Na}_v1.5$ channels. As shown in Fig. 7A, JZTX-1 ($0.5 \mu\text{M}$) delayed the $\text{Na}_v1.5$ current inactivation. This result was consistent with a previous report [17]. There was a non-competition effect with both icajine and JZTX-1; icajine ($100 \mu\text{M}$) reduced the peak current of $\text{Na}_v1.5$ channels without affecting the inactivation curve in the presence of $0.5 \mu\text{M}$ JZTX-1. In a parallel series at equivalent inhibition concentrations, icajine reduced the peak current further in the presence of TTX (Fig. 7B), indicating that there was non-competition inhibition of icajine and TTX. These results indicate that icajine neither bound to the $\text{Na}_v1.5$ channel at site 3 nor acted in a same manner as TTX. To further investigate whether the binding domain of strychnine and icajine to the $\text{Na}_v1.5$ channels involves voltage sensor trapping, we adopted a triple-pulse protocol in which a test pulse (-30 mV) following a strong depolarization ($+120$ mV) was used to measure available $\text{Na}_v1.5$ currents. As shown in Fig. 7C, $300 \mu\text{M}$ strychnine and icajine

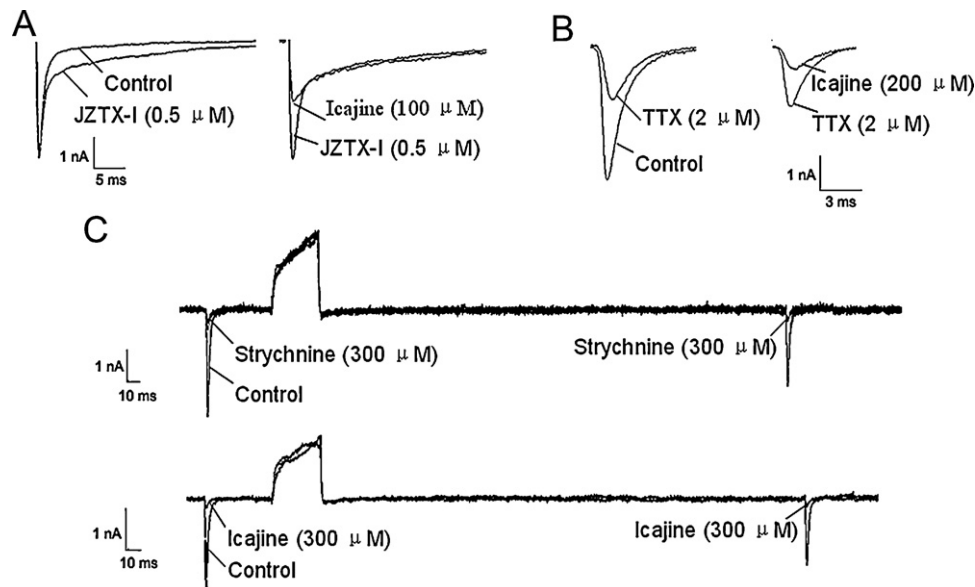


Fig. 7. Binding domain analysis for strychnine and icajine on $\text{Na}_v1.5$ channels. (A) Icajine interacts with $\text{Na}_v1.5$ channel in a different way than JZTX-1. JZTX-1 delays the inactivation of $\text{Na}_v1.5$ channels (left). Icajine reduces the peak current in the presence of JZTX-1 (right). (B) Non-competitive inhibition of the $\text{Na}_v1.5$ current between icajine and TTX. Both TTX and icajine were applied at equivalent concentrations. (C) The binding of strychnine (or icajine) to the $\text{Na}_v1.5$ channel was not dissociated by strong depolarization. Current traces were induced by a triple-pulse protocol, in which two 50 -ms test pulses of -30 mV were intervened with a 50 -ms conditioning pulse of $+120$ mV. Cells were held at -90 mV.

almost completely blocked the $\text{Na}_v1.5$ current induced by the first pulse (-30 mV). There was no more sodium current detected at the third test pulse (-30 mV), suggesting that strychnine and icajine still bind to the channels even if the sodium channels were in activation conformation.

4. Discussion

In the present study, we characterized the action of the eight alkaloid fractions extracted from the processed seeds of *S. nuxvomica* on $\text{Na}_v1.5$ channels. The pharmacological results showed that only strychnine and icajine exhibited a moderate affinity to $\text{Na}_v1.5$ channels, whereas no effect was detected for the other six analogs. Strychnine and icajine may bind to the resting state of $\text{Na}_v1.5$ channel; this is different from most local anesthetics and antiarrhythmic drugs, which block sodium channels in a use-dependent manner [18]. In particular, the study found that strychnine and icajine had little effect on steady-state fast inactivation but markedly shifted the slow inactivation of $\text{Na}_v1.5$ currents toward more hyperpolarized potentials.

The introduction of two methoxy groups on the phenyl ring to brucine as compared to strychnine caused a loss in the binding affinity for the $\text{Na}_v1.5$ channel, and a similar impairment of the $\text{Na}_v1.5$ channel inhibitory potency was noted for novacine compared to icajine. The increased bulky methoxy groups on the phenyl ring or the negatively charged oxygen atom of methoxy group may account for this lack of inhibition on the $\text{Na}_v1.5$ channel for brucine and novacine. The substitution of a large side chain on the phenyl ring may alter the optimized position for the compounds to get close to the binding sites of the channel. Breaking of the C12–O bond of brucine and strychnine, yielding compounds isobrucine and isostrychnine, respectively, resulted in a significant reduction in $\text{Na}_v1.5$ channel inhibitory potency compared to strychnine. The impairment of the ring, which produced a long side chain with a hydroxyl group at the C23-position of strychnine, would perhaps change the compact structure of strychnine and hinder the ability of the molecule to get close to the pore of $\text{Na}_v1.5$ channel. Surprisingly, strychnine-N-oxide, with the N^+ -charge fully compensated by the negatively charged oxygen atom, was inactive, indicating the importance of cationic centers for this drug–channel interaction. This was confirmed by icajine with a methyl group substitution on the nitrogen atom, which showed comparable activity to strychnine.

Strychnine and icajine reduced the $\text{Na}_v1.5$ peak currents and acted more like pore-blocking drugs. The binding sites of these compounds should be different from sites 2, 3, 5 and 6, which are the usual binding sites for drugs that produce alterations of channel inactivation, including persistent activation of sodium channels (site 2 and site 5) [19,20], slowing inactivation kinetics of sodium currents (site 3) [21], and shifting the steady-state activation and inactivation to more hyperpolarized potentials (site 6) [22,23]. The competing experiment of icajine and JZTX-I (a site 3 toxin) further confirmed that icajine binds to the $\text{Na}_v1.5$ channel, but not at site 3 domains. Strychnine and icajine showed no effect on the current–voltage relationship, and no obvious dissociation was observed with extreme strong depolarizations (Fig. 7), indicating that the mechanism of inhibition did not involve voltage sensor trapping. The competing experiment between icajine and TTX (Fig. 7) suggested that strychnine and icajine acted in a manner different than TTX.

Strychnine and icajine had little effect on the ‘steady-state fast inactivation’ curve, but shifted the ‘steady-state slow inactivation’ curve substantially, suggesting that they possibly stabilize the slow inactivated state. Slow inactivation determines sodium channel availability and thereby contributes to overall membrane excitability, determining the propensity to generate repetitive

firing and the extent of action potential back propagation. Mutations of *SCN5A* genes, which affect slow inactivation, are associated with long QT syndrome type 3 (LQT3), Brugada syndrome, primary cardiac conduction disease and idiopathic ventricular fibrillation [1]. In the present study, strychnine and icajine alter slow inactivation, indicating that they may have the potential therapeutic advantage in the above arrhythmias. However, we could not exclude the possibility that once strychnine or icajine bound to the $\text{Na}_v1.5$ channels and thus alter the slow inactivated state. In addition, strychnine is extreme toxicity and we found that the LD_{50} of strychnine is 0.37 mg/kg by intravenous administration in rats, consistent with a previous report [24]. The EC_{50} value of 83.1 μM is higher than the safe concentration. But, icajine is less toxicity and we found that the rats behaved normally after intravenous injection of icajine at the dose of 50 mg/kg. Unfortunately, the LD_{50} of icajine was not obtained because of its low solubility in saline. We therefore feel it will be important to perform additional experiments to further characterize the toxicity of icajine in the future.

Previous researches have reported that strychnine block open state of sodium channels in the squid giant axons and frog node of Ranvier which belong to nervous system [25,26]. In this study, we found that strychnine and icajine bind to a closed state of the $\text{Na}_v1.5$ channel. $\text{Na}_v1.5$ is mainly expressed in peripheral excitable tissue of cardiac muscle, which share more than 60% amino acid sequence identity with neuronal α -subunit isoforms but have differences in gating and conductance that result in distinct tissue-specific physiological functions and differences in pharmacologic properties [27]. Sodium channel blockers mediate their block by two mechanisms, resting block and use-dependent block. A hypothesis for the resting block of $\text{Na}_v1.5$ currents by strychnine and icajine was that they perhaps bind to a separate binding site apart from a common local anesthetics receptor responsible for eliciting the use-dependent block. Here we showed that strychnine and icajine block $\text{Na}_v1.5$ channel at resting state, providing evidence for the structural difference between $\text{Na}_v1.5$ and neuronal α -subunit isoforms which is related to the different binding manners.

Strychnine and icajine displayed fast association and dissociation kinetics and bind to a resting state of the $\text{Na}_v1.5$ channel. The question of how they gain access to the receptor was raised. Ahern et al. confirmed that a cation– π interaction between cationic local anesthetics and the negative electrostatic potential on the face of the aromatic rings of phenylalanine or tyrosine in the VGSCs contributes to the inhibitory mechanism [28]. Evidence for a cation– π interaction can also be insightful structurally as these interactions occur only when the cation is oriented toward the face, not the edge, of the aromatic ring in the VGSCs [29]. This prerequisite differs from the electrostatic interactions between the monopole charges of the side chains of glutamate or aspartate and lysine or arginine [30]. In this study, strychnine has N^+ -charge at the N19-position. We suppose that they bind to the channel just by orienting toward the face of the aromatic rings of phenylalanine or tyrosine with cation– π interaction; however, for brucine, novacine, isobrucine and isostrychnine, the bulky methoxy groups on the phenyl ring or the impaired compact structure probably affect the orientation. Strychnine-N-oxide, with the N^+ -charge fully compensated by the negatively charged oxygen atom, lost the activity, indicating the importance of cationic centers for the cation– π interaction.

Most of the VGSC blockers have a substituted aromatic ring as a common structural feature. It is thought to be the moiety responsible for binding to their target site [30]. In studies in which lidocaine is chemically ‘dissected’ into its hydrophilic and hydrophobic components [31], the polar, amine portion exhibits fast, use-dependent open-state blocking, while the phenolic part

exhibits less frequency-dependence in its inhibition of I_{Na} [32,33]. Strychnine and icajine are hydrophobic compounds with the phenolic part of aromatic ring. In this study, strychnine and icajine bound to the resting state of $Na_v1.5$ channels. They may bind to $Na_v1.5$ channels by cation- π interaction with a different binding site than that for local anesthetics. The conformation of the pore region changed during the binding process, but here, the allosteric model showed no influence on the affinity at resting state or depolarization state.

In conclusion, the structure-activity relationships of strychnine and its analogs on $Na_v1.5$ channels suggest that the compact structure and cationic centers are important for compounds binding to $Na_v1.5$ channels. Strychnine and icajine might interact with $Na_v1.5$ channels with a new mechanism. They bind to a certain domain of the outer vestibule of the channel pore at a different location than TTX or other pore-blocking drugs in the resting state. They markedly shifted the slow inactivation of $Na_v1.5$ currents toward more hyperpolarized potentials, which may be a therapeutic advantage in certain arrhythmias. This study would also provide information about the structure-function relationship for research on alkaloid fractions extracted from the seeds of *S. nux-vomica*.

Acknowledgements

We thank Professor Robert S. Kass for kindly providing the human $Na_v1.5$ clone. We thank Yingying Fang for technical assistance in acute toxicity studies. This work was partly supported by grants from the National Natural Science Foundation of China (No. 30900245, H00906), Key Project of Guangdong Province (No. 9351051501000003, CXZB1018) and Major State Basic Research Program of China (No. 2009CB526409).

References

- [1] Wang Q, Shen J, Splawski I, Atkinson D, Li Z, Robinson JL, et al. SCN5A mutations associated with an inherited cardiac arrhythmia, long QT syndrome. *Cell* 1995;80:805–11.
- [2] Tan HL, Bink-Boelkens MT, Bezzina CR, Viswanathan PC, Beaufort-Krol GC, van Tintelen PJ, et al. A sodium-channel mutation causes isolated cardiac conduction disease. *Nature* 2001;409:1043–7.
- [3] Abriel H. Cardiac sodium channel Nav1.5 and its associated proteins. *Arch Mal Coeur Vaiss* 2007;100:787–93.
- [4] Moraes ER, Kalapothakis E, Naves LA, Kushmerick C. Differential effects of *Tityus bahiensis* scorpion venom on tetrodotoxin-sensitive and tetrodotoxin-resistant sodium currents. *Neurotoxicol Res* 2011;19:102–14.
- [5] Veldkamp MW, Viswanathan PC, Bezzina C, Baartscheer A, Wilde AA, Balser JR. Two distinct congenital arrhythmias evoked by a multidysfunctional Na (+) channel. *Circ Res* 2000;86:E91–7.
- [6] Echt DS, Liebson PR, Mitchell LB, Peters RW, Obias-Manno D, Barker AH, et al. Mortality and morbidity in patients receiving encainide, flecainide, or placebo. The cardiac arrhythmia suppression trial. *N Engl J Med* 1991;324:781–8.
- [7] Saint DA. The cardiac persistent sodium current: an appealing therapeutic target? *Br J Pharmacol* 2008;153:1133–42.
- [8] Marbán E, Nuss HB, Donahue JK. Gene therapy for cardiac arrhythmias. *Cold Spring Harb Symp Quant Biol* 2002;67:527–31.
- [9] Moss AJ, Windle JR, Hall WJ, Zareba W, Robinson JL, McNitt S, et al. Safety and efficacy of flecainide in subjects with long QT-3 syndrome (DeltaKPQ mutation): a randomized, double-blind, placebo-controlled clinical trial. *Ann Non-invasive Electrocardiol* 2005;10:59–66.
- [10] Miura M, Yamagishi H, Morikawa Y, Matsuoka R. Congenital long QT syndrome and 2:1 atrioventricular block with a mutation of the SCN5A gene. *Pediatr Cardiol* 2003;24:70–2.
- [11] Schwartz PJ, Priori SG, Locati EH, Napolitano C, Cantu F, Towbin JA, et al. Long QT syndrome patients with mutations of the SCN5A and HERG genes have differential responses to Na channel blockade and to increases in heart rate. Implications for gene-specific therapy. *Circulation* 1995;92:3381–6.
- [12] Guizhi M. The long period clinical observation of the effect of *Strychnos nux-vomica* on Kaschin-Beck's disease. *Chinese J Regional Dis Prev Ther* 1996;11:120–4.
- [13] Jensen AA, Gharagozloo P, Birdsall NJ, Zlotos DP. Pharmacological characterization of strychnine and brucine analogues at glycine and alpha7 nicotinic acetylcholine receptors. *Eur J Pharmacol* 2006;539:27–33.
- [14] Yin W, Wang TS, Yin FZ, Cai BC. Analgesic and anti-inflammatory properties of brucine and brucine N-oxide extracted from seeds of *Strychnos nux-vomica*. *J Ethnopharmacol* 2003;88:205–14.
- [15] Liu H, Clancy C, Cormier J, Kass R. Mutations in cardiac sodium channels: clinical implications. *Am J Pharmacogenomics* 2003;3:173–9.
- [16] Kirshenbaum LA, Schneider MD. Adenovirus E1A represses cardiac gene transcription and reactivates DNA synthesis in ventricular myocytes, via alternative pocket protein- and p300-binding domains. *J Biol Chem* 1995;270:7791–4.
- [17] Xiao Y, Tang J, Hu W, Xie J, Maertens C, Tytgat J, et al. Jingzhaotoxin-I, a novel spider neurotoxin preferentially inhibiting cardiac sodium channel inactivation. *J Biol Chem* 2005;280:12069–76.
- [18] Yamagishi T, Xiong W, Kondratiev A, Vélez P, Méndez-Fitzwilliam A, Balser JR, et al. Novel molecular determinants in the pore region of sodium channels regulate local anesthetic binding. *Mol Pharmacol* 2009;76:861–71.
- [19] Linford NJ, Cantrell AR, Qu Y, Scheuer T, Catterall WA. Interaction of batrachotoxin with the local anesthetic receptor site in transmembrane segment IVS6 of the voltage-gated sodium channel. *Proc Natl Acad Sci U S A* 1998;95:13947–52.
- [20] Trainer VL, Baden DG, Catterall WA. Identification of peptide components of the brevetoxin receptor site of rat brain sodium channels. *J Biol Chem* 1994;269:19904–9.
- [21] Fletcher JI, Chapman BE, Mackay JP, Howden ME, King GF. The structure of versutoxin (delta-atracotoxin-Hv1) provides insights into the binding of site 3 neurotoxins to the voltage-gated sodium channel. *Structure* 1997;5:1525–35.
- [22] Fainzilber M, Lodder JC, Kits KS, Kofman O, Vinnitsky I, Van Rietschoten J, et al. A new conotoxin affecting sodium current inactivation interacts with the delta-conotoxin receptor site. *J Biol Chem* 1995;270:1123–9.
- [23] West PJ, Bulaj G, Yoshikami D. Effects of delta-conotoxins PVIA and SVIE on sodium channels in the amphibian sympathetic nervous system. *J Neurophysiol* 2005;94:3916–24.
- [24] Longo VG, Silvestrini B, Bovet D. An investigation of convulsant properties of the 5,7-diphenyl-1,3-diazadamantan-6-ol (IS 1757). *J Pharmacol Exp Ther* 1959;26:41–9.
- [25] Shapiro BI. Effects of strychnine on the sodium conductance of the frog node of Ranvier. *J Gen Physiol* 1977;69:915–26.
- [26] Cahalan MD, Almers W. Block of sodium conductance and gating current in squid giant axons poisoned with quaternary strychnine. *Biophys J* 1979;27:57–74.
- [27] Goldin AL. Resurgence of sodium channel research. *Annu Rev Physiol* 2001;63:671–94.
- [28] Ahern CA, Eastwood AL, Dougherty DA, Horn R. Electrostatic contributions of aromatic residues in the local anesthetic receptor of voltage-gated sodium channels. *Circ Res* 2008;102:86–94.
- [29] Ma JC, Dougherty DA. The Cationminus signpi interaction. *Chem Rev* 1997;97:1303–24.
- [30] Ahern CA, Eastwood AL, Dougherty DA, Horn R. New insights into the therapeutic inhibition of voltage-gated sodium channels. *Channels (Austin)* 2008;2:1–3.
- [31] Haeseler G, Leuwer M. Interaction of phenol derivatives with ion channels. *Eur J Anaesthesiol* 2002;19:1–8.
- [32] Haeseler G, Bufler J, Merken S, Dengler R, Aronson J, Leuwer M. Block of voltage-operated sodium channels by 2,6-dimethylphenol, a structural analogue of lidocaine's aromatic tail. *Br J Pharmacol* 2002;137:285–93.
- [33] Wallace CH, Baczkó I, Jones L, Fercho M, Light PE. Inhibition of cardiac voltage-gated sodium channels by grape polyphenols. *Br J Pharmacol* 2006;149:657–65.